WATER RESOURCES RESEARCH, VOL. 33, NO. 8, PAGES 1971–1981, AUGUST 1997

Evolution of a sediment wave in an experimental channel

Thomas E. Lisle,[1] James E. Pizzuto,[2] Hiroshi Ikeda,[3] Fujiko Iseya,[4] and Yoshinori Kodama[5]

Abstract. The routing of bed material through channels is poorly understood. We approach the problem by observing and modeling the fate of a low-amplitude sediment wave of poorly sorted sand that we introduced into an experimental channel transporting sediment identical to that of the introduced wave. The wave essentially dispersed upstream and downstream without translation, although there was inconclusive evidence of translation late in the experiment when the wave was only 10–20 grain diameters high. Alternate bars migrated through zones of differing bed load transport rate without varying systematically in volume, celerity, or transport rate. Sediment that overpassed migrating bars was apparently responsible for dispersion of the wave. The evolution of the wave was well predicted by a one-dimensional model that contains no adjusted empirical constants. Numerical experiments demonstrate, however, that the theory does not predict sediment waves that migrate long distances downstream. Such waves can only be explained by the following processes not represented by the theory: selective bed load transport, spatial variations in bar and other form roughness, the mechanics of mobile armor, and perhaps other mechanisms.

Introduction

Sediment commonly enters stream channels in uplands as large inputs from mass failure or severe surface erosion. Such inputs can create sediment waves, which we define as positive perturbations in the longitudinal distribution of channel-stored sediment that do not owe their existence solely to variations in channel morphology. We adopt the term "sediment wave" because these features can be investigated according to wave properties of celerity, amplitude, and wavelength, though natural sediment waves are characteristically nonperiodic and irregular. As sediment waves translate downstream and disperse, they transmit the signal of erosional watershed disturbances such as wildfire, land use, and climatic events to downstream channels and riparian areas. In order to predict the arrival, severity, and duration of sediment-related impacts, a better understanding of the behavior of sediment waves is needed.

There are severe impediments to studying sediment waves in natural channels. Sediment waves are described by *Gilbert* [1917], *Griffiths* [1979], *Madej* [1982], *Pickup et al*. [1983], *Beschta* [1983], *Meade* [1985], *Pearce and Watson* [1986], *Roberts and Church* [1986], *Knighton* [1989], *Maita* [1991], *Pitlick* [1993], *Turner* [1995], *Nicholas et al*. [1995], and *Madej and Ozaki* [1996], but critical information needed to develop and test quantitative models is commonly missing. The fate of large sediment inputs is most easily studied as isolated cases, but erosional events usually produce sediment from a number of sources that quickly mix in channels. Moreover, before monitoring the evolution of a wave it is vital to define its entire initial profile, but bed topography that existed before the wave was introduced is rarely known in sufficient detail.

These difficulties motivate experimentation in model channels. Previous experiments have modeled the dispersion of aggradational wedges downstream of sediment inputs [*Soni et al*., 1980; *Paola et al*., 1992; *Needham and Hey*, 1991]. These studies have provided useful data on a variety of processes but do not resolve the question of the fate of a sediment wave and its influence on processes upstream as well as downstream of the input.

We report here the results of an experiment to observe the evolution of a sediment wave of bed material introduced into a model gravel bed river. Our channel was wide enough to allow formation of alternate bars, but we did not allow banks to erode. Our results show symmetric diffusion of a stationary bed wave both upstream and downstream of the input location. We explain our observations using a simple one-dimensional theory.

Experimental Apparatus and Procedures

We conducted our experiment in the Large Flume (4 m wide × 160 m long) at the Environmental Research Center at the University of Tsukuba, Japan (Figure 1). The flume floor has a slope of 0.01 and was covered with a poorly sorted mixture of sand and fine gravel (median sieve diameter, d_{50} = 0.57 mm; graphic standard deviation = 1.2Φ) (Figure 2).

Sediment was recirculated. Outfall sediment was carried from a reservoir by buckets mounted onto a belt to a hopper, which fed another belt that returned the sediment to the head of the flume. There the sediment accumulated in a pile which was eroded laterally by the flow before entering the flume. We monitored bed elevation near the entrance of the flume during test runs before and during the experiment. Once before the experiment we added sediment to the inflow to correct an apparent deficit. Inefficient transfers of sediment in the recir-

[1]Pacific Southwest Research Station, Forest Service, U.S. Department of Agriculture, Arcata, California.
[2]Department of Geology, University of Delaware, Newark.
[3]Environmental Research Center, University of Tsukuba, Ibaraki, Japan.
[4]Department of Commercial Science, Jobu University, Gunma, Japan.
[5]Faculty of Education, Tottori University, Tottori, Japan.

Paper number 97WR01180.
0043-1397/97/97WR-01180$09.00

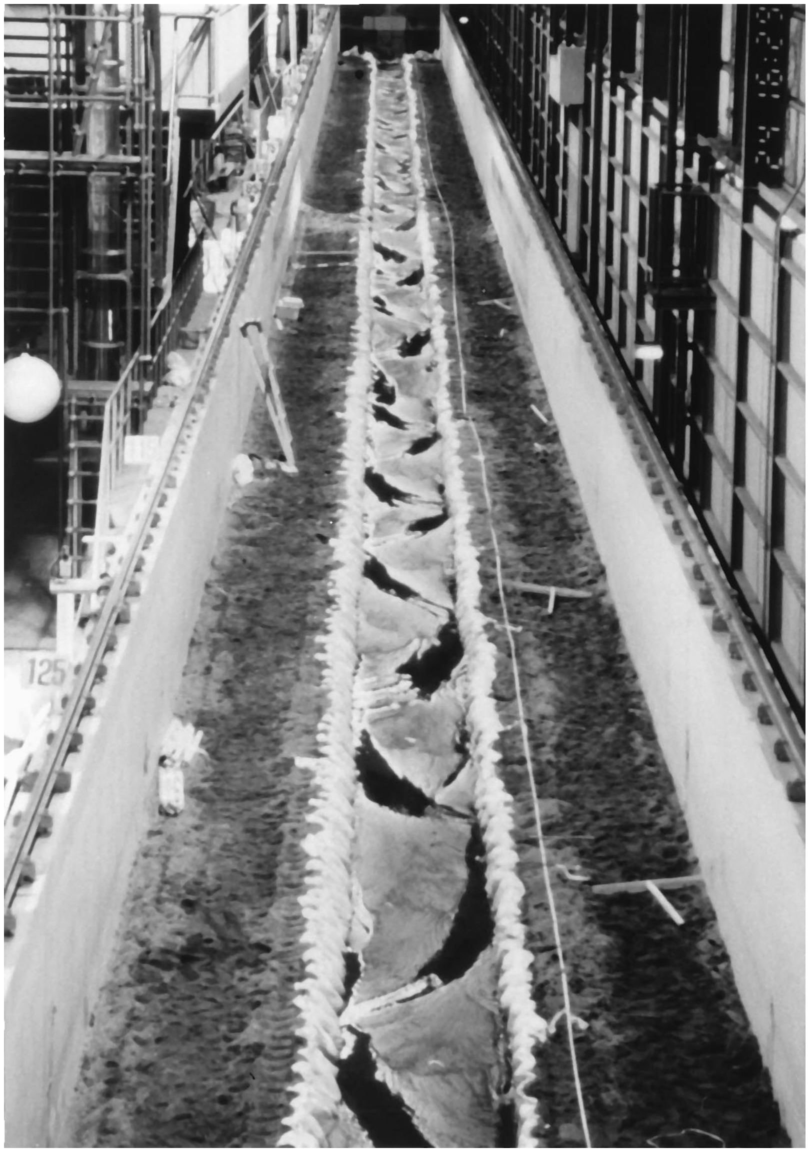

Figure 1. The Large Flume, Environmental Research Center, Tsukuba University, looking upstream after the sediment wave was introduced. The flume has been mostly drained to reveal alternate bars. The regularity of the bars in the far foreground has been disturbed by the wave.

culating system could be expected to severely dampen variations in input created by variations in sediment outfall, and we did not detect any significant changes in bed elevation near the flume entrance during the experiment.

We formed a uniform channel down the entire length of the flume and reinforced the banks with sandbags so that the final width was 1.0 m. We chose a water discharge of 8.0 L/s, which produced a mean depth of 2.0 cm, a mean velocity of 40 cm/s, a Froude number of 0.90, and a particle Reynolds number of 760. Soon after the flow was initially turned on, a continuous series of migrating alternate bars formed and occupied the entire length and width of the channel beyond a distance of about 10 m from the flume entrance. Thereafter a narrow, discontinuous band of low standing waves meandered down the thalweg.

Our intent was to model important characteristics of gravel bed channels in general but not to model any particular river. A Froude number of 1 is a theoretical upper limit for mobile bed channels when the bed is entrained, and critical flow is commonly approached during high discharges in channels with slopes of 0.01 or greater [*Grant*, 1997]. Values of width:depth ratio (50) and relative submergence (33, ratio of mean depth to d_{50}) are typical of gravel bed rivers with alternate bars [*Ikeda*, 1975]. The River Ystwyth, a straightened gravel bed channel with alternate bars that initially migrated until sinuosity developed [*Lewin*, 1976], may serve as an unintended prototype; in the Ystwyth at bank-full stage, width:depth ratio was 17, relative submergence was roughly 70, and channel gradient was 0.0037.

We designed our experiment to allow alternate bars to form so that sediment could disperse laterally and the resulting sediment storage could affect longitudinal dispersion as it might in a natural channel. However, alternate bars in gravel bed channels rarely migrate unless the channel is straight, bed material is relatively uniform, and channel gradient is low [*Church and Jones*, 1982; *Lisle et al.*, 1991].

After bed elevations and bar dimensions beyond the 10-m entrance section were approximately uniform we cast sediment over a 20-m section of channel from 60 to 80 m downstream of the flume entrance during a 45-min period as the system ran. We distributed the input as a triangular wave; the initial wave's apex was ~4 cm high. The rate of input was about 10 times the background bed load transport rate (described below) and resulted in rapid deposition of an initial sediment wave. The sediment (800 kg, 0.52 m^3 bulk volume) had the same particle-size mixture as the original bed. During the input, bars continued to migrate through the input section.

After the sediment wave was introduced, we continued to hold water discharge steady, recirculate sediment, and measure changes in bed topography until the sediment wave disappeared. As the system ran, we monitored the location of migrating bar fronts down the entire flume length at 15-min intervals and measured sediment outfall rate at 10-min intervals. On six occasions we shut the system down to sketch maps and to measure bed topography with a point gage. Bed elevations were measured at 0.5-m intervals down three longitudinal profiles; one located over the center line, and the other two located half the distance to either bank. We measured bed topography in greater detail by probing the bed thickness at 40 cross sections from 90 to 110 m, and in the same reach we measured water surface profiles at 10 to 20 cross sections before each shutdown.

Results

Mean Bed Load Transport Rates

Bed load transport rates were relatively high throughout the experiment. Sediment outfall rates over 10-min intervals averaged 0.038 kg/s (dry weight; standard deviation = 0.0062 kg/s). Mean dimensionless bed load transport rate

$$W^* = \frac{\left(\frac{\rho_s - \rho}{\rho}\right) q_s}{g^{1/2}(hS)^{3/2}}$$

(where $\rho_s = 2.65$ g/cm^3 is sediment density, ρ is water density, q_s is volumetric transport rate per unit channel width, g is gravitational acceleration, h is water depth, and S is energy gradient) was high relative to values for natural channels. The value for W^* equaled 4.3, which is well into the highest range of *Parker*'s [1990] function for bed load transport rate. In this range, pavements are expected to disappear. We sampled the bed surface at the end of the experiment by scraping a layer a few grain diameters thick at three locations in the channel. The average of these distributions showed a slight coarsening of the surface layer (Figure 2).

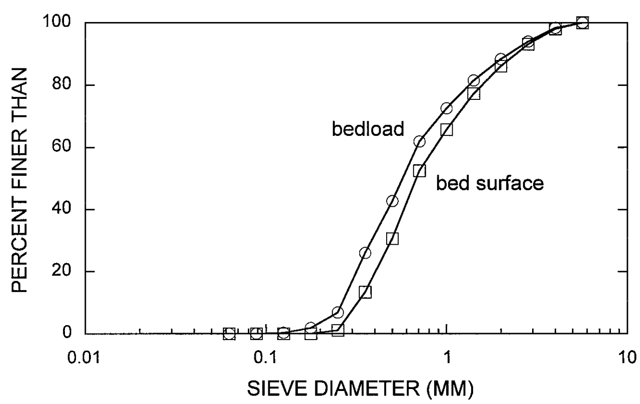

Figure 2. Particle-size distributions of bed load and bed-surface material.

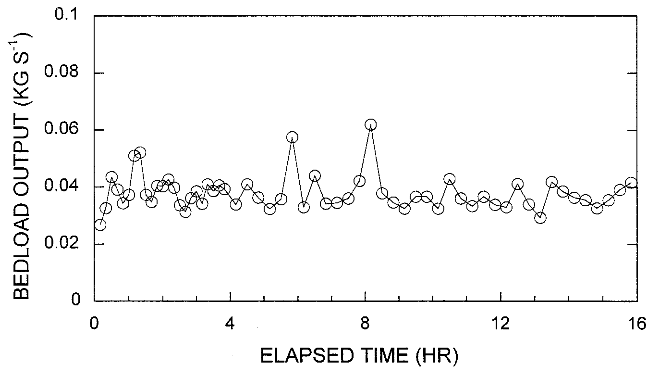

Figure 3. Bed load outfall rates.

Variations in sediment outfall rates showed no systematic rises and falls that would indicate passage of a sediment wave (Figure 3) but instead were produced by exiting alternate bars. As presented later, bed load transport by bar migration accounted for the majority of total bed load transport. Bed load transport generally increases toward the downstream limit of a migrating bar or bed form. Given a characteristic bar wavelength (3.5 m) and migration rate (0.7 m per 10 min), each outfall sample would contain only a portion of a single bar as it exited the flume. Despite the fact that outfall rates did not register the exit of the front of the wave from the flume, some of the wave may have recirculated back to the flume entrance. The wave constituted 7.2% of total bed material, which was 3.4% less at the end of the experiment than that after the wave was introduced, suggesting that approximately one half of the wave was stored in the recirculation system at the end of the experiment.

Evolution of the Sediment Wave

Longitudinal variations in bed elevation above the flume floor showed alternate bars with wavelengths of 2–5 m superimposed over the sediment wave, which had an initial wavelength of 20 m (Figure 4). To distinguish the wave from the alternate bars, we computed the volume of sediment stored in each 5-m channel segment (using the three longitudinal profiles) and divided by the area of each segment (5 m^2) to obtain the mean bed thickness or elevation relative to the flume floor.

We offer two interpretations of changes in bed thickness

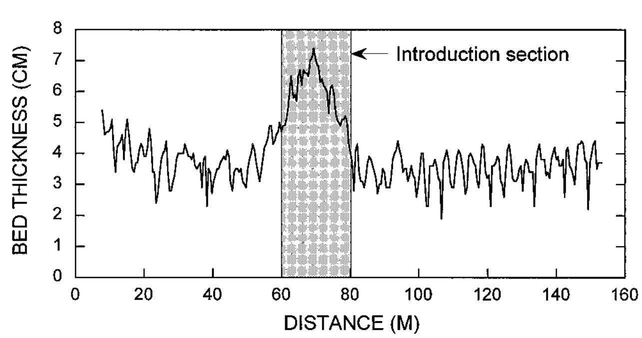

Figure 4. Unsmoothed centerline profile at 0.75 hours.

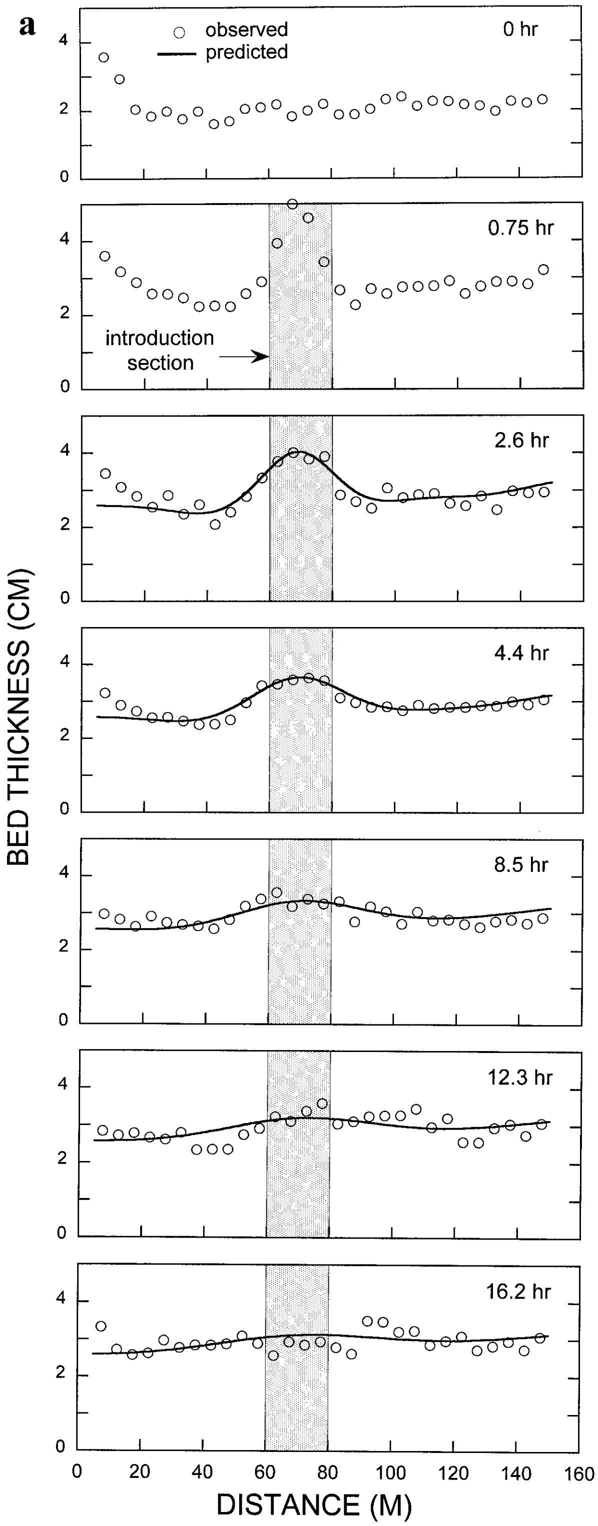

Figure 5. Downstream variation in bed thickness averaged over 5-m channel segments. (a) Measured bed thickness and values predicted from a one-dimensional model of bed evolution. (Observations at distances between 0 and 20 m were neglected in applying the one-dimensional model.) (b) Autocorrelation coefficients. (c) Difference in measured values between succeeding intervals. Here, "s.e." is the average standard error of the mean of bed elevations in a 5-m segment.

with respect to evolution of a sediment wave. According to a "first-order" interpretation the introduced wave essentially remained in place for 12 hours as it dispersed and eventually disappeared (Figure 5a). Dispersion was accomplished by erosion of the wave crest, deposition of eroded sediment downstream, and trapping of incoming sediment upstream. The wave disappeared during the last interval ending at 16.2 hours. The standard deviation for mean bed elevations measured over 5-m segments (σ_5) equaled 2 mm before the wave was introduced, increased to 8 mm in the first interval afterward, and did not decline to the original value until the last interval. Our modeling, which is presented later, best represents this first-order interpretation.

To test objectively the presence of a wave and to evaluate changes in wave length throughout the experiment, we examined autocorrelations of 5-m mean bed thicknesses at a range of separating distances (lags) from 5 to 70 m (Figure 5b). For reference, approximate 95% confidence limits are shown for autocorrelations under the hypothesis of an independent series. Before the wave was introduced, there were no significant autocorrelations beyond a lag of 5 m. After the wave was introduced, there was a zone of negative autocorrelation centered at about 25 m, which apparently corresponded to the initial wave. In subsequent intervals up to the last the zone of negative correlation shifted to larger lags apparently as the wave dispersed. Autocorrelations were lower in the last interval, except for a single significant negative autocorrelation at 35 m that was not part of a wider pattern. Autocorrelations support the first-order interpretation of the existence of a dispersing wave that disappears in the last interval. This analysis does not test wave translation.

However, if one uses the previous bed profile as the datum for each succeeding profile (by subtracting the later profile from the earlier), then a "second-order" interpretation emerges that includes a possible downstream-migrating wave (Figure 5c). In agreement with the first-order interpretation, there was erosion of the introduced wave and deposition upstream and downstream during the first three intervals after the wave was introduced (0.75–8.5 hours). During the next interval (8.5–12.3 hours) the bed eroded upstream of the midpoint of the original wave (70 m) and filled downstream, signaling the downstream translation of the wave. The pattern of erosion and deposition may have shifted downstream in the final interval, but there was also an unexplained region of fill upstream of 60 m, and the standard deviation of variation in mean bed thickness (σ_5 = 2.3 mm; Figure 5a) was only slightly greater than that (σ_5 = 2.0 mm) before the wave was introduced.

We do not claim that a translating wave existed in the last two intervals but instead offer the second-order interpretation to entertain the possibility of its existence. Its amplitude was intermediate between particle and bar scales. Specifically, wave amplitude (~10 mm) during these intervals was 18 times d_{50} and less than one-half mean bar amplitude (23 mm). Nevertheless, a wave amplitude of 10 mm is much greater than the standard error (1.4 mm) of the estimate of the mean bed thickness in 5-m channel segments, and therefore it appears to have been a significant feature.

Bars

We constructed a wide experimental channel in order to allow the sediment wave to be affected by lateral sediment dispersion over bars. However, as described later in this paper, a one-dimensional model satisfactorily predicts the observed evolution of the wave; thus it was not necessary to explicitly model two-dimensional features and processes. Nevertheless, it was important to investigate how dispersion occurred and, more specifically, how it was affected by variations in sediment transport associated with bar migration.

Total bed load transport in any section of the channel was the sum of "bar" transport (the volume moved by migrating bars) and "throughput" transport (the volume that passed over migrating bars without being captured and overridden). *Lewin* [1976] observed both bar transport and throughput transport in the River Ystwyth.

We computed bar transport rate as the product of bar volume per unit channel length and bar celerity. Average transport rates were computed for six run intervals between seven shutdowns. We measured bar volume from the three longitudinal profiles surveyed after each shutdown. To do this, we identified the upstream and downstream lows that marked the endpoints of each bar in each profile. The portion of bar volume for each profile equaled the product of the longitudinal area above a straight line drawn between the two endpoints and one third of the channel width (0.30 m); total bar volume equaled the sum of the three subvolumes. To test the accuracy of this method, we also measured bar volumes from detailed transverse soundings of bed thickness from 90 to 110 m. From these data we constructed 10 longitudinal profiles at 10-cm intervals across the bed and computed bar volume as before. The mean difference between 3-profile and 10-profile measurements of bar volumes was ±27%. We believe this error justifies only broad interpretations of downstream patterns of

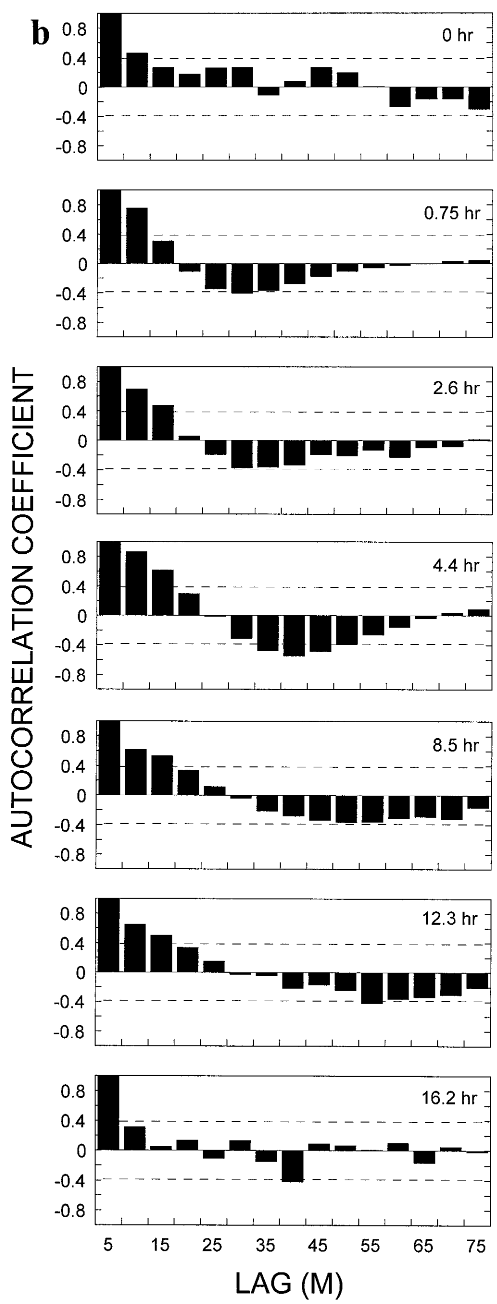

Figure 5. (continued)

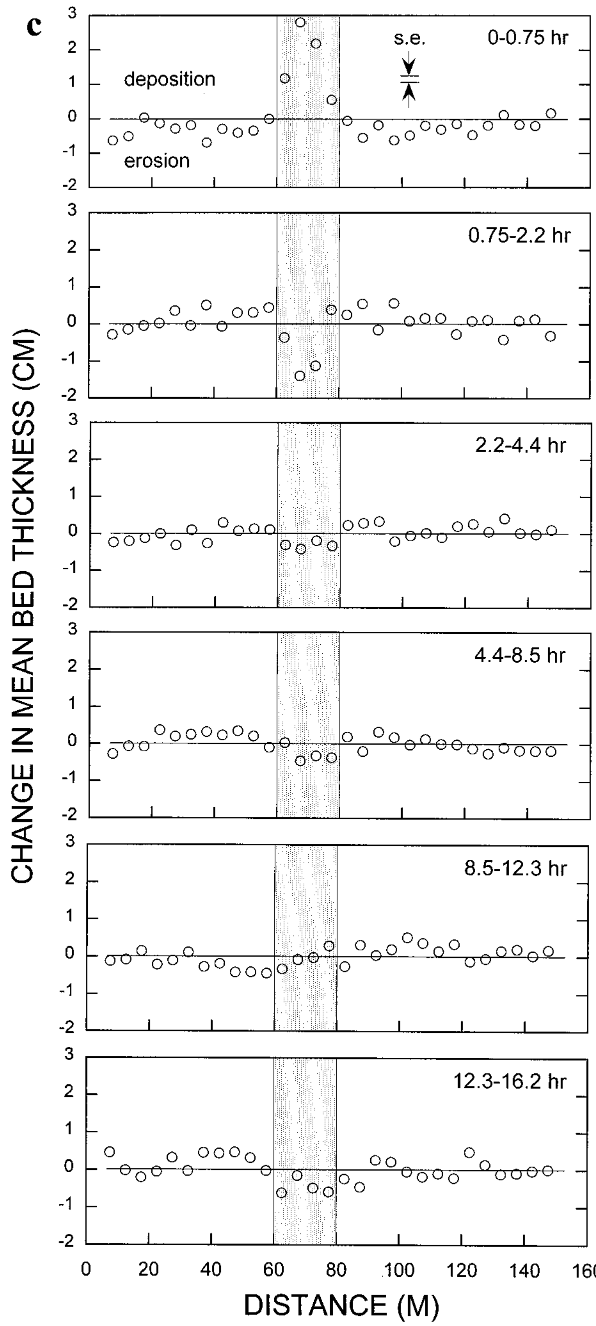

Figure 5. (continued)

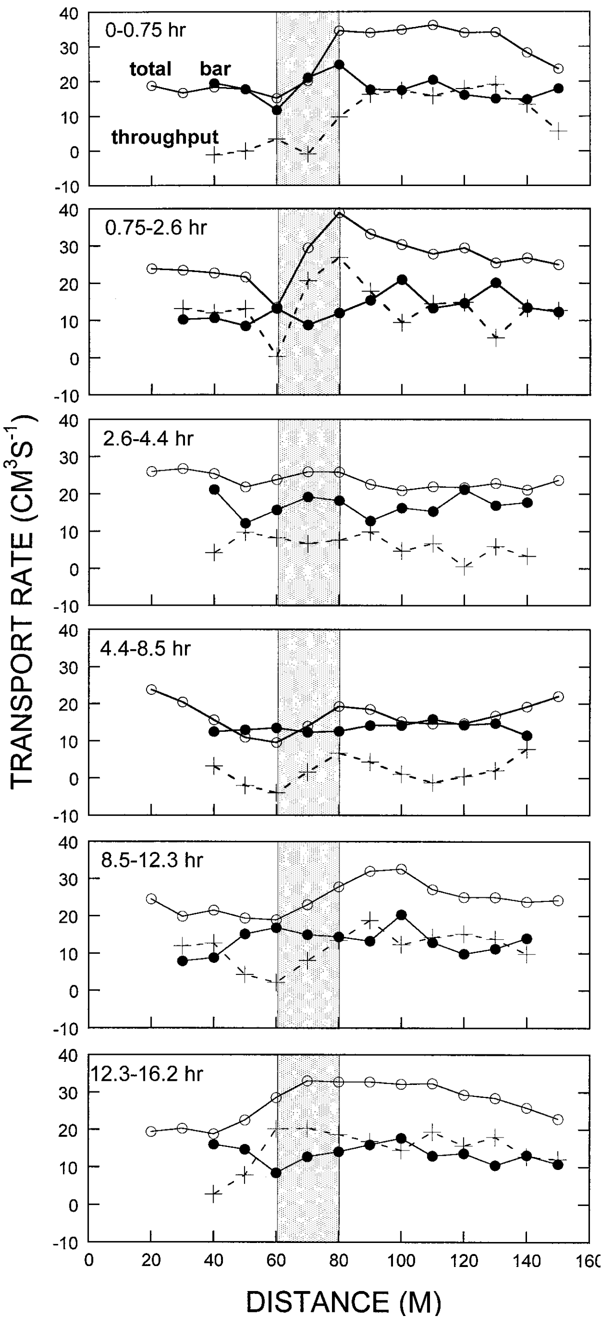

Figure 6. Streamwise variations in total, bar, and throughput bulk bed load transport rates. Shaded area marks location of sediment introduction. Some points for bar and throughput transport near upstream and downstream ends of the flume appear to be missing because of migration of bars into and out of the 150-m measurement section during a run interval.

bar and throughput transport rates. We measured bar celerity from the locations of migrating bar fronts that we marked at ~15-min intervals. We used longer 10-m segments in these computations in order to smooth variations in segment-averaged bar transport rates.

We also computed the total local bulk transport rate (Q_s) for 10-m-long segments during each run interval by solving the finite difference form of the one-dimensional equation of sediment continuity

$$\frac{\partial n}{\partial t} = -\frac{1}{1-p}\frac{\partial Q_s}{\partial x} \tag{1}$$

where n is the local bed elevation, t is time, p is the porosity of the bed, and x is the downstream coordinate. Using an assumed porosity of 0.4, we converted the average sediment outfall rate to a bulk rate (24 cm^3/s) and assumed this to be the input rate at the first section (10–20 m). We computed the output at the end of the section from the change in storage (obtained from the change in average bed elevation). Values of Q_s for downstream sections were computed similarly. Throughput transport equals total transport minus bar transport.

Longitudinal variations in total transport rate reflect erosion of the wave and deposition upstream and downstream (Figure 6). During the interval after wave introduction (0.75–2.6 hours), transport rate declined approaching the wave, signifying increasing deposition. Downstream, transport increased and peaked over the eroding wave and decreased more gradually farther downstream as the rate of deposition attenuated. The pattern of increasing transport rates in the vicinity of the introduced wave and decreasing transport rates upstream and downstream was repeated in later intervals, although with greater variation around this general pattern as the experiment progressed. This pattern was maintained in the interval from 8.5 to 12.3 hours when, according to the second-order interpretation, the wave shifted downstream (Figure 5c). The small variation in total transport at the downstream end of the channel is consistent with a similar lack of variation in sediment outfall rates (Figure 3).

Bar transport rate and bar volume (not shown) varied widely both spatially and temporally but did not appear to be related to longitudinal variations in total sediment transport. Bar transport rates averaged 14–18 cm^3/s, and throughput transport rates averaged 7 cm^3/s. Patterns of variation in throughput transport resembled those in total transport, but bar transport rates did not show a consistent pattern. This suggests that bars were conservative features that did not respond as they migrated through changing zones of sediment transport. Instead, variations in sediment transport created by the wave were predominantly transmitted by sediment particles bypassing sequences of burial and erosion associated with bar migration.

Theory of Sediment Wave Deformation

Many mathematical models of river bed profile evolution caused by bed load transport processes are described in the literature [*Cui et al.*, 1996; *deVries*, 1973; *Gradowczyk*, 1968; *Gill*, 1988; *Lai*, 1991; *Pickup et al.*, 1983; *Ribberink and Van der Sande*, 1985; *Weir*, 1983; *Vreugdenhil*, 1982; *Zhang and Kahawita*, 1987, 1988]. Previous studies, however, do not provide a convenient means of analyzing our experimental data, and therefore we present our own mathematical model below. The formulation presented here is not particularly new, but our numerical solutions provide considerable insight into our experimental data in particular and sediment wave evolution in general.

The first equation needed to develop the theory is a one-dimensional fluid momentum conservation equation

$$\frac{\partial}{\partial x}\left(\frac{u^2}{2g} + h + n\right) = \frac{\partial H}{\partial x} = -\frac{\tau}{\rho g h} \tag{2}$$

where u is the vertically averaged fluid velocity, τ is the total boundary shear stress exerted by the flow, and H is the total mechanical energy of the fluid per unit weight, defined by the sum of the velocity, elevation, and pressure heads (Figure 7). The boundary shear stress is related to the local flow velocity using a spatially constant friction coefficient, C_f

$$\tau = \rho C_f u^2 \tag{3}$$

Assuming a steady flow and uniform width, the continuity equation for the fluid is

$$q = uh \tag{4}$$

where q is the unit discharge. The continuity equation for bed load transport has already been introduced (equation (1)), although unit transport rates (q_s) are substituted for total rates (Q_s).

Before introducing a bed load transport equation we observe that in general the total shear stress, τ, may be partitioned into grain and form roughness components

$$\tau = \tau_G + \tau_B \tag{5}$$

where τ_G represents the shear stress exerted on the sediment grains and τ_B represents the shear stress exerted on bed undulations such as bars or other form roughness elements. We use the method of *Parker and Peterson* [1980] to compute τ_G, which is more directly related to sediment transport rates. The friction coefficient associated with surface particles is found by using a form of the law of the wall

$$C_G = \kappa^2\left(\ln \frac{z}{z_0}\right)^{-2}$$

(where κ = von Karman's constant equal to 0.40 and z_0 = the height above the bed where velocity is projected to go to zero). For mean velocity, $z = 0.368\ h$, and we substitute $z_0 = 0.1d_{84}$ [*Whiting and Dietrich*, 1990]. Assuming uniform flow, we obtain $\tau = \rho g h S$ from (2). The channel slope influenced by grains (S_G) is found by using (3) and factoring C_G by Froude number [$Fr = u(gh)^{-1/2}$] and slope

$$C_G = Fr^{-2} S_G \tag{6}$$

Finally, we use (3) to compute τ_G, which was equal to 18.5 dyne cm^{-2}, or 89% of the total boundary shear stress. These calculations indicate that form roughness was a relatively small fraction of total roughness. Therefore we neglect τ_B below and consider the total shear stress τ to be equal to τ_G. This also implies that C_f is approximately equal to C_G.

An equation for bed load transport is required to close (1)–(5). A simple form of the Meyer-Peter-Muller equation is used here [*Sinha and Parker*, 1996]

$$q_s = K(R_s g d_s)^{1/2} d_s (\tau_G^*)^{3/2} \tag{7}$$

where K is a dimensionless constant, R_s is the submerged specific gravity of sediment, d_s is particle diameter which we represent by the median sieve size (d_{50}), and

$$\tau_G^* = \frac{\tau_G}{g(\rho_s - \rho) d_{50}} \tag{8}$$

In adopting (7) we have not included the critical shear stress required to initiate bed load motion. Thus (7) is only valid for stresses far in excess of that required for bed load motion. In our experiment, τ_G^* equaled 0.20, which exceeds the conventional values assigned to critical shear stress by more than 3 times. With $K = 8$ [*Sinha and Parker*, 1996] the equation

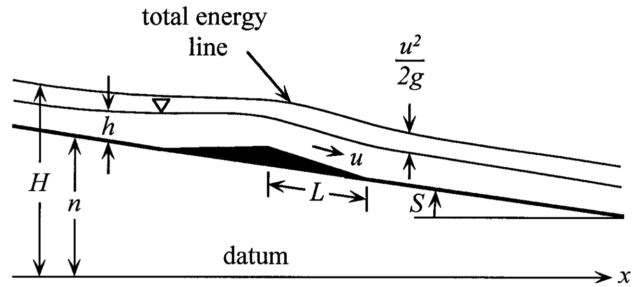

Figure 7. Definition of variables for analysis of one-dimensional bed evolution.

predicts a unit bulk transport rate of 0.69 cm^2/s, or ~3 times the mean measured rate of 0.23 cm^2/s. This amount of error is common for bed load equations, and the presence of bars and a wide range of grain sizes may depart from the conditions under which the equation was formulated.

To derive an equation for the evolution of the bed topography during our experiment, (1)–(5), (7), and (8) are combined and rearranged. This requires several steps, which are outlined below.

1. Eliminate τ_G from the bed load transport equation using (3) and (8) to obtain bed load transport rate in terms of $C_f u^3$

$$q_s = \frac{K C_f^{1/2} C_f u^3}{R_s g} \tag{9}$$

2. Substitute (9) into the sediment continuity equation (1) to eliminate q_s. For convenience later, also divide and multiply the right side by q

$$\frac{\partial n}{\partial t} = -\frac{K C_f^{1/2} q}{R_s(1-p)} \frac{\partial}{\partial x}\left(\frac{C_f u^3}{gq}\right) \tag{10}$$

3. Substitute the fluid continuity equation (4) and the resistance equation (3) into the momentum equation (2) and rearrange to obtain an equation for $C_f u^3/gq$

$$-\frac{\partial H}{\partial x} = \frac{C_f u^3}{gq} \tag{11}$$

4. Substitute (11) for $C_f u^3/gq$ in (10)

$$\frac{\partial n}{\partial t} = \frac{K q C_f^{1/2}}{R_s(1-p)} \frac{\partial^2 H}{\partial x^2} \tag{12}$$

5. A more convenient form of (12) can be obtained by first defining a uniform flow over a plane bed of slope S that would exist before the addition of a sediment wave, similar to the equilibrium channel that initially existed in our flume. Such a uniform flow would have a depth h_0, a velocity u_0, a total bed stress $\tau_0 = \rho g h_0 S$, and a Froude number $Fr_0 = u_0(gh_0)^{-1/2}$. Using (6), $C_f^{1/2}$ can be written as $S^{1/2} Fr_0^{-1}$. Substituting this result into (12) yields the final equation for the evolution of bed topography

$$\frac{\partial n}{\partial t} = \frac{K q S^{1/2}}{R_s(1-p) Fr_0} \frac{\partial^2 H}{\partial x^2} \tag{13}$$

According to (13) the rate of change in bed elevation is proportional to the curvature of the total energy line (Figure 7).

Table 1. Summary Statistics Describing the Differences Between the Bed Elevations Predicted by the Model and the 5-m Average Bed Elevations From Our Experiment

Elapsed Time, hours	Mean Error, cm	Standard Deviation, cm	Maximum Error, cm
2.6	0.00029	0.22	0.47
4.4	0.0023	0.12	0.28
8.5	0.010	0.19	0.38
12.3	0.011	0.25	0.48
16.2	0.012	0.24	0.48

Maximum error is an absolute value.

Application of the Theory to our Experiment

To apply (13) to our experiment, initial and boundary conditions need to be defined. We started our computations using the bed profile (smoothed at 5-m intervals) obtained after the sediment wave was introduced, thereby defining the necessary initial condition. The appropriate boundary conditions should specify a static bed elevation far upstream and downstream of the sediment wave. In order to achieve this, the domain for the computations was extended upstream and downstream an additional 20 m beyond the physical limits of the flume, far enough that the added sediment would not influence bed elevations at the upstream and downstream ends of the domain.

A simple numerical procedure was used to solve (13). The equation was discretized using a standard explicit finite difference approximation on a uniform spatial grid of 0.5 m. The time steps were typically very small, as required by well-known considerations of numerical stability. The variables u and h, needed to determine H at the grid points, were obtained from a standard step-backwater computation performed before solving (13) at each time step [*French*, 1985].

The theory was applied to our experimental results using the following parameters: $p = 0.4$, $Fr_0 = 0.9$, $q = 8$ L/s, and $S = 0.01$. None of the parameters were adjusted in any way during the computations. The predicted profiles follow the experimental data without large systematic deviations (Figure 5a). The root-mean-square error of predicted bed elevations at 5-m intervals (0.12–0.25 cm; Table 1) was approximately equal to the standard deviation of 5-m mean bed elevations that were measured before the wave was introduced and during the last interval when it was mostly dispersed (0.20–0.23 cm). This indicates that predicted bed elevations replicated the trend of measured bed elevations within the background variation during evolution of the wave.

The theory apparently provides a mechanistic explanation for our first-order interpretation, as the predicted profiles essentially decay in place without significant migration either upstream or downstream. The theory does not reproduce our second-order interpretation of potential wave migration between 8.5 hours and 12.3 hours.

Application of the Theory to Wave Deformation in General

We performed two sets of numerical experiments to determine if significant wave migration could be predicted by the theory for conditions different from those of our experiment. To facilitate comparison with our experimental results, all of the numerical experiments adopted a channel width of 1 m, a discharge of 8 L/s, a porosity of 0.4, and sediment and water densities of 2.65 and 1.0 g/cm^3 (note that the grain size of the sediment does not appear in our theory). In all the experiments a sediment wave was placed as a symmetrical, triangular perturbation on a plane bed (as illustrated in Figure 7); the wavelength of the wave, L, was defined as one half of the length of its base. One set of experiments was performed with a slope of 0.01; the initial height of the triangular wave was kept fixed at $0.5h_0$. The friction coefficient was allowed to vary, thus particle size cannot expected to be constant. Another set of experiments was performed with a slope of 0.001, and the initial height of the triangular wave was kept fixed at $0.05h_0$. For each set of experiments the Froude number was varied from 0.1 to 1.5, and the initial wavelength of the sediment wave was varied from 1 m to 20 m. Before calculations began, the initial triangular wave was smoothed slightly using a five-point moving average.

In order to quantify the extent of wave migration and dispersion a Peclet number was computed for each numerical experiment. The Peclet number is a dimensionless parameter frequently used in numerical methods and heat transport problems to quantify the relative strengths of advection and diffusion [*Koutitas*, 1983]. It is defined by

$$Pe = vL/D$$

where v is the velocity of the center of mass of the sediment wave (defined as the distance moved by the center of mass during the simulation, divided by the duration of the simulation) and D is a sediment wave diffusion coefficient

$$D = \frac{\sigma_f^2 - \sigma_i^2}{2t}$$

where σ^2 is the variance of the bed elevations (the bed elevation here is measured relative to the sloping equilibrium bed), t is the duration of the experiment, and the subscripts f and i refer to the end and the beginning of the numerical experiment, respectively.

Results of three runs are presented in Figure 8 to illustrate the variety of forms created as the waves evolve under differing conditions. At a Froude number of 0.5 the triangular wave moves steadily downstream but becomes progressively lower in amplitude and longer in wavelength; the Peclet number for this numerical experiment is 0.037. At a Froude number of 0.9 the wave mostly decays in place, with a slight downstream migration of the center of mass; the Peclet number is 1.4×10^{-5}. At a Froude number of 1.5 the wave migrates upstream, while also becoming longer in wavelength and lower in amplitude; the Peclet number is -0.0046. The upstream migration of the wave in supercritical flow may at first seem counterintuitive. However, the results obtained here are analogous to the upstream migration of antidunes in supercritical flow. Furthermore, upstream migration of sediment waves in supercritical flow has been predicted by theoretical treatments [*Gradowczyk*, 1968; *Lai*, 1991], so the results presented here should not be surprising.

The Peclet numbers obtained during the two sets of numerical experiments are illustrated as mesh diagrams in Figure 9. For Froude numbers greater than or equal to about 0.5 the Peclet number is effectively zero, indicating that under these conditions sediment waves will decay rapidly without significant migration. When the Froude number is around 0.1 and the wavelength is around 5 m (for $S = 0.001$) or 1 m (for $S = 0.01$), the Peclet number rises to maximum values between 0.2 and 0.3. These Peclet numbers, though local maxima, still indicate a dominance of diffusion over advection, and thus even under these conditions, sediment waves will tend to spread rapidly as they migrate downstream. Apparently, the simple one-dimensional theory developed in this paper cannot predict the existence of a persistent sediment wave that migrates far downstream. *Cui and Parker* [1997], using a linearized stability analysis applicable to low-amplitude sediment waves, present a similar conclusion.

Discussion

Our theory explains our experimental results well, although the possible wave migration at the end of the experiment is not reproduced by the theory. Furthermore, extensive numerical experiments apparently do not detect a persistent, migrating sediment wave under any reasonable Froude number or initial wavelength. This appears to contradict some field observations and apparently negates our initial hypothesis that wave migration is an important process of unsteady bed load transport in rivers.

Our theory, however, essentially includes only one factor that could influence the evolution of a sediment wave (longitudinal variations in bed slope), despite other factors being significant in our experiment and still others likely to be important in nature (spatial variations in bar morphology, selective transport and attrition of bed particles, or longitudinal variations in sediment supply and transport capacity). Therefore results obtained here do not negate the possibility of sediment wave migration. Rather, they indicate that changes in longitudinal bed slope alone (and their influence on flow hydraulics and transport rates) are insufficient to cause significant translation of sediment waves.

Our theory, however, explains the broad pattern of wave evolution observed, suggesting that variations in longitudinal bed slope were of paramount importance in our experiment.

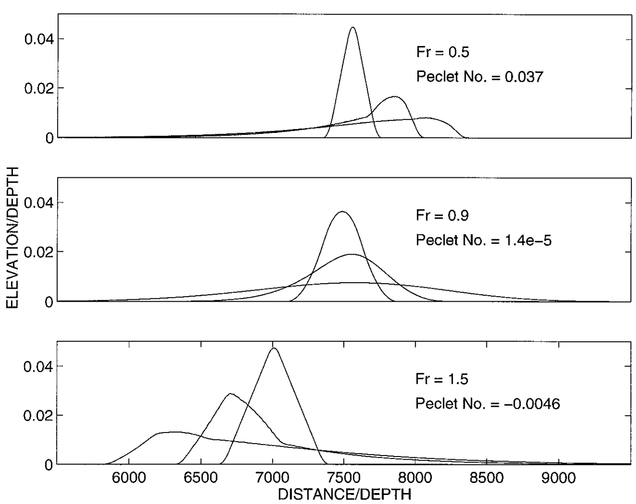

Figure 8. Calculations illustrating the evolution of triangular bed waves. The initial wavelength (5 m), water discharge (8 L/s), sediment density (2.65 g/cm^3), bed porosity (0.4), and slope (0.001) are held constant. The depth used to scale the horizontal and vertical axes is h_0. The elevation is defined relative to the sloping bed of the preexisting equilibrium channel. The highest amplitude wave in each plot is the initial form. Progressively lower forms indicate the morphology of the wave at the following times: 4.6 and 9.2 hours ($Fr = 0.5$), 1.4 and 10.5 hours ($Fr = 0.9$), and 5.3 and 14.1 hours ($Fr = 1.5$).

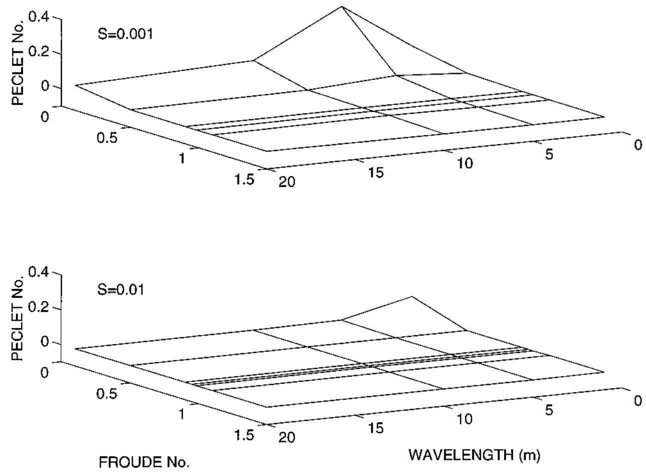

Figure 9. Peclet number for sediment wave evolution as a function of Froude number and initial wavelength for $S = 0.001$ and $S = 0.01$.

This is not surprising, as the sediment wave we created was a very large one, with an amplitude of 2–3 times the mean depth of the preexisting equilibrium channel. Only near the end of the experiment, when the wave had decayed to a small fraction of its initial amplitude and variations in longitudinal bed slope were small, did we observe evidence of sediment wave migration (albeit inconclusive).

These observations suggest a speculative conceptual model for the evolution of large sediment waves similar to the one modeled by our laboratory experiment. Initially, variations in longitudinal slope will be the dominant influence on wave evolution, and the sediment wave will decay in amplitude and grow longer in wavelength without significant migration upstream or downstream. After the sediment wave has decayed significantly, other influences may predominate and cause the wave to migrate downstream as a persistent and coherent feature.

Unfortunately, it is difficult to evaluate these hypotheses using available field data. Case studies that provide comprehensive and detailed data on sediment waves in natural channels are lacking, and therefore, at best we can evaluate only qualitatively the relative degrees of diffusion and translation for a few natural waves. Another problem is that experimental conditions are likely to deviate from those in nature in subtle ways. For example, recirculating sediment-feed systems typically impose relationships between bed surface texture and bed load transport rates that differ from those in natural channels [*Parker and Wilcock*, 1993]. As a result of using a recirculating system, starting with an unpaved, smooth bed, and applying dimensionless boundary shear stresses that exceeded the threshold for initial motion of bed particles by more than threefold, we attained high bed load transport rates. The resulting poorly developed pavement severely limited any response of bed surface texture to wave-related variations in load or transport capacity. Different results might have been observed if we had used a sediment-feed system [*Dietrich et al.*, 1989; *Kuhnle*, 1989; *Lisle et al.*, 1993], and still different results might be anticipated in nature.

Nonetheless, it is still instructive to compare experimental results with field data, and therefore we have selected four field examples to evaluate our hypothesis that diffusion will pre-

Table 2. Characteristics of Sediment Waves in Four Natural Channels

	$\frac{\text{Amplitude}}{\text{Bank-Full Depth}}$	$\frac{\text{Amplitude}}{\text{Wavelength}}$	$\frac{(d_{50})_{\text{wave}}}{(d_{50})_{\text{bed}}}$	Translation
Fall River	1	6×10^{-4}	0.1[a]	yes, no
Redwood Creek	≥1[b]	10^{-5}[c]	≤1[d]	uncertain
Navarro River	2	4×10^{-3}	>1[e]	no
East Fork River	<0.5	5×10^{-4}	0.3[f]	yes

[a]Bed material is pavement.
[b]Wide and uncertain range of values for entire sediment wave including reaches upstream of recent zone of aggradation.
[c]Order-of-magnitude value for entire wave. Large value in part caused by dispersed sediment sources.
[d]Fining of bed accompanies aggradation.
[e]Range of material sizes in wave is wider than preexisting bed.
[f]Wave material is bed load collected downstream of tributary; bed material is from subsurface samples from same reach [*Leopold and Emmett*, 1976, 1977; *Emmett*, 1980].

dominate over translation where sediment waves are large and where variations in slope are the predominant influence on wave evolution. Not surprisingly, our experimental conditions of high sediment transport rates, lack of mobile armor, absence of size-selective transport, and uniform flow are poorly met by available field examples.

In 1982, a dam break flood severely eroded the Roaring River channel in Colorado and deposited a fan of 280,000 m^3 of coarse material that filled 500 m of Fall River, a low-gradient meandering channel having a gravel pavement [*Pitlick*, 1993]. During the subsequent nival flood, 25,000 m^3 of sandy material was eroded from the fan and formed a wave that moved down Fall River and filled the channel from ~2000 to 3500 m downstream from the fan. In subsequent years the wave decayed in place behind a meander cutoff that apparently stopped further wave migration.

In 1955, 1964, 1972, and 1975, large volumes of gravel and sand were delivered to Redwood Creek, northern California, during severe floods from hillslopes that were disturbed by logging and road building [*Janda et al*., 1975]. Widespread sediment sources caused aggradation in most of the main channel, which is ~100 km long. From 1973 (when monumented cross sections were established) to 1988, mean streambed elevation decreased in the upper 80 km of channel and increased in the lower 20 km [*Madej and Ozaki*, 1996]. This suggests the downstream translation of a sediment wave, although bed elevation changes before 1973 are not well known, and bed elevations over much of the channel apparently remained higher in 1988 than they were before the sediment inputs. It is not clear, therefore, to what degree recent aggradation in downstream reaches represents arrival of a translating wave or extension of the leading front of a spreading wave (M. A. Madej, U.S. Geological Survey, personal communication, 1997).

In 1995 a 80,000 m^3 landslide created an 8-m high dam on the Navarro River, a 30-m wide gravel bed channel in northwestern California. Within hours, after the dam was overtopped and partially breached, a wedge of coarse material was deposited as far as 400 m downstream [*Hansler et al*., 1996]. High flows during the following year caused 24,000 m^3 of scour of the sediment wedge, but the center of mass and zone of maximum thickness did not shift downstream. Although landslide material was found farther downstream of the initial deposits, the topographic front of the wave did not advance because of severe particle attrition of the soft landslide material. At the same time, a wedge of river gravel was deposited upstream of the pond left by the partially breached dam.

Sediment waves in the East Fork River, Wyoming, are clearly translational. They are produced annually by inputs of sandy bed load from a tributary into the paved, gravel bed channel of the East Fork that, above the junction, transports little sandy material [*Andrews*, 1979; *Meade*, 1985]. These waves are 500–600 m long, contain the mean annual bed load yield of 2500–3000 Mg, and typically traverse 500 m during the annual nival flood. Sediment waves over a 4-km study reach downstream of the tributary appear to migrate downstream with little dispersion [*Meade*, 1985].

In summary, the field examples show a variety of behavior from being clearly stationary (Navarro) to clearly translational (East Fork) or showing evidence for either (Fall and Redwood) (Table 2). The wave in the Navarro most closely resembles that in our flume in terms of its behavior, dimensions, and particle size. The translational waves (including the translational phase of the Fall River wave) fill channels no higher than their banks and are composed of material that is much finer than preexisting bed material.

The selected cases we present do not refute the predictions of our model. However, more field studies are needed to identify and evaluate important factors that affect behavior of natural sediment waves. Experimentation, with interpretations from theoretical models, provides a strategic approach to isolating and quantifying effects of those factors.

Conclusions

A sediment wave that we introduced into a laboratory channel did not translate significantly downstream but instead diffused both upstream and downstream, as sediment that was eroded from the introduced wave was deposited downstream and incoming sediment was trapped upstream of the wave. As alternate bars migrated through zones of differing sediment transport rate that were created by wave dispersion, the bars showed no systematic response in volume, celerity, or transport rate. Diffusion of the wave was apparently accomplished by sediment that overpassed the bars without being captured. Despite the presence of two-dimensional bed features the evolution of the wave was well represented by a one-dimensional model containing no adjusted empirical coefficients. The model predicts that wave celerity will be low relative to diffusivity where variations in longitudinal slope predominate in affecting wave evolution.

Acknowledgments. We gratefully acknowledge Hideji Maita, Akio Hara, Tomomi Nakamura, Akio Nakano, Mutsuhito Suzuki, and Yei Wei for assisting us in the experiment, and Thembi Borras, Sue Hilton, and Jack Lewis for analyzing data. Yantao Cui, Dick Iverson, and Jon Nelson offered helpful comments that improved our theory. Reviews by Mike Church, Gordon Grant, and Leslie Reid greatly improved our paper.

References

Andrews, E. D., Hydraulic adjustment of the East Fork River, Wyoming to the supply of sediment, in *Adjustments of the Fluvial System*, edited by D. D. Rhodes and G. P. Williams, pp. 69–94, Kendall/Hunt, Dubuque, Iowa, 1979.

Beschta, R. L., Channel changes following storm-induced hillslope erosion in the Upper Kowai Basin, Torlesse Range, New Zealand, *N. Z. J. Hydrol*., *22*(2), 93–111, 1983.

Church, M., and D. Jones, Channel bars in gravel-bed rivers, in *Gravel-Bed Rivers*, edited by R. D. Hey, J. C. Bathurst, and C. R. Thorne, pp. 291–324, John Wiley, New York, 1982.

Cui, Y., and G. Parker, Linear analysis of coupled equations for sediment transport, in *International Association for Hydraulic Research, 27th Congress, Water for a Changing Global Community*, Am. Soc. of Civ. Eng., New York, in press, 1997.

Cui, Y., G. Parker, and C. Paola, Numerical simulation of aggradation and downstream fining, *J. Hydraul. Res.*, *34*, 185–203, 1996.

deVries, M., River-bed variations—Aggradation and degradation, in *Proceedings of the International Seminar on Alluvial Streams*, Int. Assoc. for Hydraul. Res., Delft, Netherlands, 1973.

Dietrich, W. E., J. W. Kirchner, H. Ikeda, and F. Iseya, Sediment supply and the development of the coarse surface layer in gravel-bedded rivers, *Nature*, *340*, 215–217, 1989.

Emmett, W. W., A field calibration of the sediment-trapping characteristics of the Helley-Smith bed load sampler, *U.S. Geol. Surv. Prof. Pap.*, *1139*, 44, 1980.

French, R. H., *Open Channel Hydraulics*, 705 pp., McGraw-Hill, New York, 1985.

Gilbert, G. K., Hydraulic mining debris in the Sierra Nevada, *U.S. Geol. Surv. Prof. Pap.*, *105*, 154, 1917.

Gill, M. A., Hyperbolic model for aggrading channels, *J. Hydraul. Eng.*, *114*(7), 1245–1255, 1988.

Gradowczyk, M. H., Wave propagation and boundary instability in erodible bed channels, *J. Fluid Mech.*, *33*, 93–112, 1968.

Grant, G. E., Critical flow constrains flow hydraulics in mobile-bed streams: A new hypothesis, *Water Resour. Res.*, *33*(2), 349–358, 1997.

Griffiths, G. A., Recent sedimentation history of the Waimakriri River, New Zealand, *N. Z. J. Hydrol.*, *18*(1), 6–28, 1979.

Hansler, M. E., D. G. Sutherland, S. J. Hilton, and T. E. Lisle, Initial evolution of a coarse sediment wave, Navarro River, California (abstract), *EOS Trans. AGU*, *77*(46), Fall Meet. Suppl., F253, 1996.

Ikeda, H., On the bed configuration in alluvial channels: Their types and condition of formation with reference to bars, *Geogr. Rev. Jpn.*, *48*(10), 712–730, 1975.

Janda, R. J., K. M. Nolan, D. R. Harden, and S. M. Coleman, Watershed conditions in the drainage basin of Rewood Creek, Humboldt County, California, as of 1973, *U.S. Geol. Surv. Open File Rep.*, *75-568*, 266, 1975.

Knighton, A. D., River adjustments to changes in sediment load and the effects of tin mining on the Ringarooma River, Tasmania, 1875–1984, *Earth Surf. Processes Landforms*, *14*, 233–246, 1989.

Koutitas, C. G., *Elements of Computational Hydraulics*, 138 pp., Pentech, London, 1983.

Kuhnle, R. A., Bed-surface size changes in gravel-bed channel, *J. Hydraul. Eng.*, *115*(6), 731–743, 1989.

Lai, C., Modeling alluvial-channel flow by multimode characteristics method, *J. Eng. Mech.*, *117*, 32–53, 1991.

Leopold, L. B., and W. W. Emmett, Bedload measurements, East Fork River, Wyoming, *Proc. Natl. Acad. Sci. U. S. A.*, *73*(4), 1000–1004, 1976.

Leopold, L. B., and W. W. Emmett, 1976 bedload measurements, East Fork River, Wyoming, *Proc. Natl. Acad. Sci. U. S. A.*, *74*(7), 2644–2648, 1977.

Lewin, J., Initiation of bed forms and meanders in coarse-grained sediment, *Geol. Soc. Am. Bull.*, *87*, 281–285, 1976.

Lisle, T. E., H. Ikeda, and F. Iseya, Formation of stationary alternate bars in a steep channel with mixed-size sediment: A flume experiment, *Earth Surf. Processes Landforms*, *16*, 463–469, 1991.

Lisle, T. E., F. Iseya, and H. Ikeda, Response of a channel with alternate bars to a decrease in supply of mixed-size bed load: A flume experiment, *Water Resour. Res.*, *29*(11), 3623–2629, 1993.

Madej, M. A., Sediment routing and channel changes in an aggrading stream in the Puget Lowland, Washington, *Gen. Tech. Rep. PNW Pac. Northwest For. Range Exp. Stn.*, *141*, 97–108, 1982.

Madej, M. A., and V. Ozaki, Channel response to sediment wave propagation and movement, Redwood Creek, California, USA, *Earth Surf. Processes Landforms*, *21*, 911–927, 1996.

Maita, H., Sediment dynamics of a high gradient stream in the Oi River Basin of Japan, *Gen. Tech. Rep. PSW Pac. Southwest For. Range Exp. Stn.*, *GTR-130*, 56–64, 1991.

Meade, R. H., Wavelike movement of bedload sediment, East Fork River, Wyoming, *Envir. Geol.*, *7*(4), 215–225, 1985.

Needham, D. J., and R. D. Hey, On nonlinear simple waves in alluvial river flows: A theory for sediment bores, *Philos. Trans. R. Soc. London A*, *334*, 25–53, 1991.

Nicholas, A. P., P. J. Ashworth, M. J. Kirkby, M. G. Macklin, and T. Murray, Sediment slugs: Large scale fluctuations in fluvial sediment transport rates and storage volumes, *Prog. Phys. Geogr.*, *19*(4), 500–519, 1995.

Paola, C., G. Parker, R. Seal, S. Sinha, J. B. Southard, and P. R. Wilcock, Downstream fining by selective deposition in a laboratory flume, *Science*, *258*, 1757–1760, 1992.

Parker, G., Surface-based bedload transport relation for gravel rivers, *J. Hydraul. Res.*, *28*, 417–436, 1990.

Parker, G., and A. W. Peterson, Bar resistance of gravel-bed streams, *J. Hydraul. Div. Am. Soc. Civ. Eng.*, *106*(HY10), 1559–1575, 1980.

Parker, G., and P. R. Wilcock, Sediment feed and recirculating flumes: Fundamental difference, *J. Hydraul. Eng.*, *119*(11), 1193–1204, 1993.

Pearce, A. J., and A. J. Watson, Effects of earthquake-induced landslides on sediment budget and transport over a 50-yr period, *Geology*, *14*, 52–55, 1986.

Pickup, G., R. J. Higgins, and I. Grant, Modelling sediment transport as a moving wave—The transfer and deposition of mining waste, *J. Hydrol.*, *60*, 281–301, 1983.

Pitlick, J., Response and recovery of a subalpine stream following a catastrophic flood, *Geol. Soc. Am. Bull.*, *105*, 657–670, 1993.

Ribberink, J. S., and J. T. M. Van der Sande, Aggradation in rivers due to overloading—Analytical approaches, *J. Hydraul. Res.*, *23*, 273–284, 1985.

Roberts, R. G., and M. Church, The sediment budget in severely disturbed watersheds, Queen Charlotte Ranges, British Columbia, *Can. J. For. Res.*, *16*, 1092–1106, 1986.

Sinha, S. K., and G. Parker, Causes of concavity in longitudinal profiles of rivers, *Water Resour. Res.*, *32*(5), 1417–1428, 1996.

Soni, J. P., R. J. Garde, and K. G. Ranga Raju, Aggradation in streams due to overloading, *J. Hydraul. Div. Am. Soc. Civ. Eng.*, *106*(HY1), 117–132, 1980.

Turner, T. R., Geomorphic response of the Madison River to point sediment loading at the Madison Slide, southwest Montana, M.S. thesis, 99 pp., Mont. State Univ., Bozeman, 1995.

Vreugdenhil, C. B., Numerical effects in models for river morphology, in *Engineering Applications of Computational Hydraulics*, vol. 1, edited by M. B. Abbott and J. A. Cunge, pp. 91–110, Pitman, London, 1982.

Weir, G. J., One-dimensional bed wave movement in lowland rivers, *Water Resour. Res.*, *19*(3), 627–631, 1983.

Whiting, P. J., and W. E. Dietrich, Boundary shear stress and roughness over mobile alluvial beds, *J. Hydraul. Eng.*, *116*(2), 1495–1511, 1990.

Zhang, H., and R. Kahawita, Nonlinear model for aggradation in alluvial channels, *J. Hydraul. Eng.*, *113*(3), 353–369, 1987.

Zhang, H., and R. Kahawita, Nonlinear hyperbolic system and its solutions for aggraded channels, *J. Hydraul. Res.*, *26*, 323–342, 1988.

H. Ikeda, Environmental Research Center, University of Tsukuba, Ibaraki 305, Japan. (e-mail: ikeda@src2.suiri.tsukuba.ac.jp)

F. Iseya, Department of Commercial Science, Jobu University, Gunma 372, Japan.

Y. Kodama, Faculty of Education, Tottori University, Tottori 680, Japan. (e-mail: kodama@fed.tottori-u.ac.jp)

T. E. Lisle, Pacific Southwest Research Station, Forest Service, U.S. Department of Agriculture, 1700 Bayview Drive, Arcata, CA 95521. (e-mail: tel7001@axe.humboldt.edu)

J. E. Pizzuto, Department of Geology, University of Delaware, Newark, DE 19716. (e-mail: pizzuto@brahms.udel.edu)

(Received May 28, 1996; revised April 3, 1997;
accepted April 15, 1997.)